

# A quasi-radial stability criterion for rotating relativistic stars

Kentaro Takami,<sup>1\*</sup> Luciano Rezzolla<sup>1,2</sup> and Shin'ichirou Yoshida<sup>3</sup>

<sup>1</sup>Max-Planck-Institut für Gravitationsphysik, Albert-Einstein-Institut, Am Mühlenberg 1, D-14476 Golm, Germany

<sup>2</sup>Department of Physics, Louisiana State University, Baton Rouge, LA 70802, USA

<sup>3</sup>Department of Earth Science and Astronomy, Graduate School of Arts and Sciences, University of Tokyo, Japan

Accepted 2011 June 1. Received 2011 June 1; in original form 2011 May 16

## ABSTRACT

The stability properties of relativistic stars against gravitational collapse to black holes is a classical problem in general relativity. In 1988, a sufficient criterion for secular instability was established by Friedman, Ipser & Sorkin, who proved that a sequence of uniformly rotating barotropic stars are secularly unstable on one side of a turning point and then argued that a stronger result should hold: that the sequence should be stable on the opposite side, with the turning point marking the onset of secular instability. We show here that this expectation is not met. By computing in full general relativity the F-mode frequency for a large number of rotating stars, we show that the neutral-stability point, that is, where the frequency becomes zero, differs from the turning point for rotating stars. Using numerical simulations, we validate that the new criterion can be used to assess the dynamical stability of relativistic rotating stars.

**Key words:** black hole physics – relativistic processes – methods: numerical – stars: neutron – stars: oscillations – stars: rotation.

## 1 INTRODUCTION

The stability of a relativistic star against gravitational collapse to a black hole is one of the most important predictions of general relativity (GR). While this problem is reasonably well understood for non-rotating stars (Misner, Thorne & Wheeler 1973), this is not the case for rotating stars and is particularly obscure when the stars are rapidly rotating. A milestone in this landscape is the criterion for secular stability proposed by Friedman, Ipser & Sorkin (1988), who proved that a sequence of uniformly rotating barotropic stars are secularly unstable on one side of a turning point (an extremum of mass along a sequence of constant angular momentum or an extremum of angular momentum along a sequence of constant rest mass). They then argued, based on an expectation that viscosity leads to uniform rotation, that the turning point should identify the onset of secular instability. While for a non-rotating star, the turning point coincides with the secular-instability point (and with the dynamical-instability point for a barotropic star if the perturbation satisfies the same equation of state of the equilibrium model), for rotating stars, it is only a sufficient condition for secular instability. Lacking other guides, the turning point is routinely used to find dynamical instability in simulations (Baiotti et al. 2005; Radice, Rezzolla & Kellerman 2010).

Our understanding of the dynamical instability of relativistic stars in uniform rotation can be improved by determining the neutral-stability line, that is, the set of stellar models whose frequency of the fundamental mode of quasi-radial oscillation (F mode)

is vanishingly small. While this problem is challenging from a perturbative point of view, especially when the rate of rotation becomes high, it can be tackled through numerical calculations. We have therefore simulated in full GR 54 stellar models and calculated accurately the corresponding F-mode frequency via a novel analysis of the power spectral density (PSD) of the central rest-mass density. This new approach has been validated through a comparison with all the available data, showing excellent agreement and, most importantly, a much smaller variance. By construction, in fact, simulations cannot evolve models at (or near) the neutral-stability line, but the accuracy of our F-mode frequencies and their smooth dependence on the central rest-mass density and dimensionless rotation rate have allowed us to produce an analytic fit of the data and deduce from this the neutral-stability line. We find in this way that it coincides with the turning point for spherical stars, but not for rotating stars, with the difference increasing with the angular momentum. Although somewhat surprising, this difference is not in contrast with the predictions of the turning-point criterion, since the latter is only a sufficient condition for secular instability and not a necessary condition for secular and dynamical instabilities. Hence, a stellar model which is stable according to the turning-point criterion can be nevertheless dynamical unstable.

To test the new stability line and validate whether it can be used to mark the threshold for dynamical stability, we have evolved stellar models whose properties fall in a small region near the two stability lines. Special attention has been paid to stellar models that are predicted to be stable by the turning-point criterion but unstable by the neutral-stability line. Because these models indeed collapse to black holes, we conclude that the neutral-stability line can be used effectively to mark the boundary to dynamical instability.

\*E-mail: kentaro.takami@aei.mpg.de

The organization of the Letter is as follows. Section 2 describes the numerical setup and initial data, while Section 3 presents our approach to extract the eigenfrequency and offers comparisons with previous work. Section 4 collects our results and a comparison between the two stability criteria, leaving the conclusions to Section 5. Unless stated differently, we use units in which  $c = G = M_{\odot} = 1$ .

## 2 NUMERICAL SETUP AND INITIAL DATA

All of our calculations have been performed in full GR using the `Whisky2D` code described in detail in Kellerman et al. (2008). This is a two-dimensional code based on the three-dimensional `Whisky` code (Baiotti et al. 2005), and exploiting the condition of axisymmetry through the ‘cartoon’ method (Alcubierre et al. 2001). In essence, the evolution of the space–time is obtained using the two-dimensional version of `Ccatie`, a finite-differencing code providing the solution of a conformal traceless formulation of the Einstein equations (Pollney et al. 2007), while the equations of relativistic hydrodynamics are solved for a flux-conservative formulation of the equations, as first discussed in detail in Baiotti et al. (2005). The `Whisky2D` code implements a variety of approximate Riemann solvers and several reconstruction methods and, as discussed in Giacomazzo, Rezzolla & Baiotti (2009), the use of reconstruction schemes of order high enough is fundamental for an accurate evolution. In particular, the results presented here have been computed using the piecewise-parabolic reconstruction method (Colella & Woodward 1984), the HLLC approximate Riemann solver (Harten, Lax & van Leer 1983) and a third-order Runge–Kutta method for the time-evolution.

The initial equilibrium stellar models are built using the `rns` code (Stergioulas & Friedman 1995) as isentropic, uniformly rotating, relativistic, perfect-fluid polytropes with the equation of state

$$p = K \rho^{\Gamma}, \quad e = \rho + \frac{p}{\Gamma - 1}, \quad (1)$$

where  $p$  is the pressure,  $\rho$  is the rest-mass density,  $K$  is the polytropic constant,  $\Gamma$  is the polytropic exponent and  $e$  is the energy density. Although all the results can be rescaled for any choice of  $K$  and  $\Gamma$ , here, we have set  $K = 100$  and  $\Gamma = 2$ , which yield stars with the maximum gravitational mass  $M = 1.64 M_{\odot}$  for a non-rotating star and  $M = 1.88 M_{\odot}$  for a uniformly rotating one. The `rns` code provides an equilibrium solution in spherical polar coordinates after specifying for each stellar model a central density  $\rho_c$ , and a equatorial and a polar (coordinate) radius in a ratio  $r_p/r_e$ . Once this solution is found, it is mapped to a Cartesian grid of `Whisky2D` and used as initial data for the subsequent evolution. Attention needs to be paid that the resolution in the calculation of the initial data matches well the one used in the evolution. We have verified that a resolution of  $(n_r, n_{\theta}) = (2001, 2601)$  [ $(n_r, n_{\theta}) = (1001, 1301)$ ], with  $(n_r, n_{\theta})$  the number of points of the radial and angular grids of the `rns` code, is needed for an accurate evolution in the high [low]-resolution setup of the `Whisky2D` code. Furthermore, because we are not interested here in extracting gravitational-wave information, we place the outer boundary at a few stellar radii and use a uniform grid with spacing  $\Delta x = \Delta z = h$  ranging between  $h = 0.04 M_{\odot}$  for the rapidly rotating models and  $h = 0.1 M_{\odot}$  for the slowly rotating ones. As done in Kellerman et al. (2008), we stagger the grid in the  $x$ -direction of half a cell. A large number of tests have been carried out to verify that the results do not depend on the position of the outer boundary, or on the value of the density in the atmosphere (see Baiotti et al. 2005), which we set to be 9 orders of magnitude smaller than the central one.

As discussed by many authors (Font, Stergioulas & Kokkotas 2000; Font et al. 2002; Baiotti et al. 2005), the truncation error in the initial data is sufficient to trigger perturbations in the star, which will start to oscillate in a number of eigenmodes. However, because we need to determine the eigenfrequency of the F mode, it is important that as much as possible of the initial perturbation energy goes into exciting that mode. For this reason we introduce an initial perturbation using the eigenfunction of the F mode for a non-rotating neutron star with the same central density, and which can be computed from linear perturbation theory (PT). More specifically, denoting by  $\psi_{\text{TOV}}$  any fluid quantity of the non-rotating model with the same central density and with  $\delta\psi_{\text{TOV}}(r)$  the corresponding eigenfunction with  $r$  the radial coordinate in the isotropic coordinate system, we approximate the equivalent eigenfunction for a rotating star in a coordinate system  $(r, \theta)$  as  $\delta\psi(r, \theta) = \delta\psi_{\text{TOV}}[rR_{\text{TOV}}/R(\theta)]$ , where  $R_{\text{TOV}}$  is the radius of the non-rotating star and  $R(\theta)$  that of the rotating star, which will obviously depend on the angle  $\theta$ . As a result, the power in the initial perturbation is mostly concentrated in the F mode, whose corresponding peak in the PSD of any hydrodynamical quantity is larger by at least a factor of 10 than any other mode. As an additional validation of the procedure, we have computed the numerical eigenfunction for some selected models and verified that it matches very well the guessed one even in the case of rapidly rotating stars and long-term evolutions.

## 3 METHODOLOGY AND ACCURACY

As customary, we extract the F-mode frequency by performing a discrete Fourier transform of the evolution of a representative hydrodynamical quantity, such as the central rest-mass density  $\rho_c$ , and by inspecting the corresponding PSD. Defining as  $F_N$  the frequency of the largest peak in the numerical PSD, previous studies determined the value of the F-mode frequency,  $F$ , by fitting the PSD with a known analytic function (e.g. a Lorentzian, Kellerman et al. 2008) or by taking the derivative of the PSD (Zink et al. 2010). The frequency obtained in these ways depends sensitively on the fitting function used, on the shape of the PSD around  $F_N$  and on the evolution time  $\tau$ . We here use a different approach. Because  $F_N$  will tend to  $F$  as the evolution time  $\tau \rightarrow \infty$ , we simply consider the evolution of  $F_N$  for increasingly large values of  $\tau$ . What we find in this way is that  $F_N(\tau)$  is an oscillating function around  $F$ , whose amplitude is, however, bounded by two envelopes which have a clear  $1/\tau$  dependence. Fitting for these envelopes and extrapolating for  $\tau \rightarrow \infty$ , we obtain a very accurate and possibly optimal value for  $F$ . As we will discuss in the following section, this approach turns out to give an excellent measure of the F-mode eigenfrequency and we recommend it in all those studies aimed at determining eigenfrequencies of relativistic stars.

### 3.1 Comparison with previous works

The F-mode frequency of spherical stars can be computed to arbitrary precision within a linear perturbative approach (see Yoshida & Eriguchi 2001, and references therein). Hence, as a first validation of the accuracy of our procedure, we have estimated the F-mode frequency for 14 non-rotating models with  $\rho_c \in [3.0 \times 10^{-4}, 3.0 \times 10^{-3}]$ ; in this range, the F mode first grows, then reaches a maximum and finally decreases to zero at the secular-instability point, around  $\rho_c \approx 3.18 \times 10^{-3}$ . Defining the relative error as  $\sigma_{\text{rel}} \equiv [(F)_{\text{PT}}^2 - (F)^2]/(F)_{\text{PT}}^2$ , where  $F_{\text{PT}}$  and  $F_N$  are, respectively, the frequencies of the F mode from PT and from our simulation. The relative error is extremely small at low densities

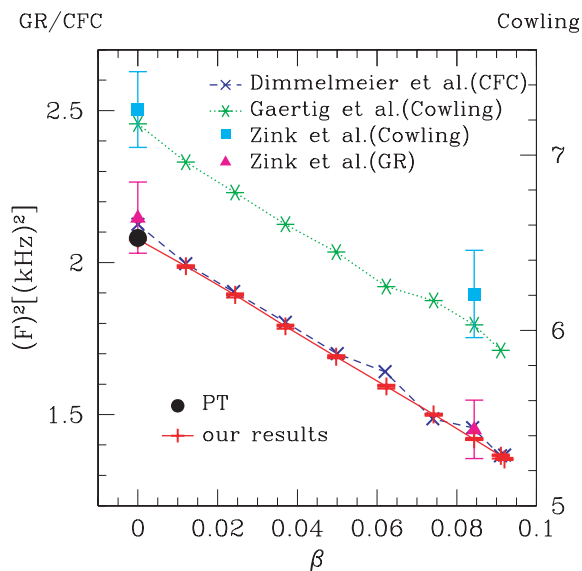


**Figure 1.** Comparison of our F-mode frequencies with those of previous works in either PT, the CFC approximation (Dimmelmeier, Stergioulas & Font 2006), the Cowling approximation (Gaertig & Kokkotas 2008; Zink et al. 2010) or in full GR (Zink et al. 2010).

[e.g.  $\sigma_{\text{rel}} \lesssim 0.005$  for  $\rho_c \approx (0.3\text{--}1.5) \times 10^{-3}$ ] and it increases with the density [e.g.  $\sigma_{\text{rel}} \lesssim 0.05$  for  $\rho_c \approx (2.5\text{--}3.0) \times 10^{-3}$ ], becoming of the order of about 10 per cent at the edge of the secular instability. This is obviously due to the fact that as  $F_N \approx 0$ , numerical calculations become increasingly long and inaccurate.

We next compare our numerical estimates for the F-mode frequency with those made in several different approaches and approximations, using as a reference a central rest-mass density  $\rho_c = 1.28 \times 10^{-3}$ , as this is the one most commonly used. We start our comparison by considering the case of non-rotating stars, for which results are available from the works of Dimmelmeier et al. (2006) or of Zink et al. (2010), in either the conformally-flat condition (CFC) or in full GR, respectively. This is shown in Fig. 1, which reports the F-mode frequency as a function of the dimensionless ratio  $\beta \equiv T/|W|$  between the rotational kinetic energy  $T$  and the binding energy  $W$ . Note that the frequency is reported in two different scales, referring to simulations either in full GR/CFC (left-hand scale) or in the Cowling approximation (right-hand scale), which systematically yields larger frequencies. Although the CFC (blue crosses) for a non-rotating star should give the same frequency in full GR (magenta filled triangles and red crosses) and in PT (black filled circle), Fig. 1 shows that this is not quite the case, although the differences are only of  $\sim 2$  per cent. Considerably larger are instead the differences with the frequencies in the Cowling approximation, which are larger by a factor of  $\sim 3$  (green stars and light-blue filled squares). Clearly, the difference between the results in full GR and the perturbative ones is much smaller, and indeed the one with our new results is the smallest among all the data available. We also note that our results also report the estimated error bars, which are much smaller than the size of the symbols.

Considering next the comparison also for rotating stars, it is easy to see that our results in two dimensions match well those in three dimensions of Zink et al. (2010) for the rotation rates available and obviously have smaller error bars. The very good match with the results in the CFC (Dimmelmeier et al. 2006), with differences of a few per cent only for all the values of  $\beta$ , confirms the conclusions drawn by Dimmelmeier et al. (2006) that the CFC is a

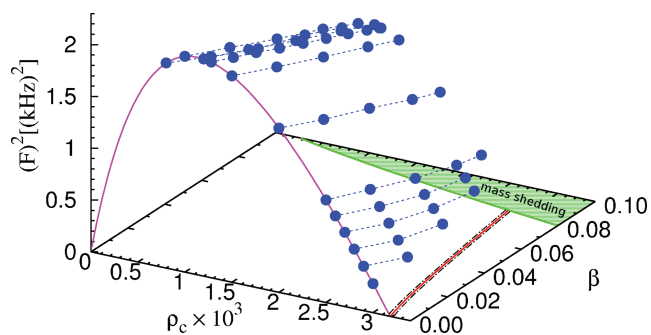


**Figure 2.** Square of the F-mode frequencies (blue filled circles) as a function of  $\rho_c$  and  $\beta$ . The dashed green area shows models above the mass-shedding limit and the red solid line marks the neutral stability (cf. Fig. 3).

very good approximation, at least for the dynamics of isolated stars. Fig. 1 also shows that the comparison with frequencies computed in the Cowling approximation (Gaertig & Kokkotas 2008; Zink et al. 2010) is considerably worse. Besides an intrinsic difference between the two sets of data (the frequencies of Gaertig & Kokkotas 2008 are in agreement only within the error bars of Zink et al. 2010), the rate of change in the frequencies with  $\beta$  differs from the one found in full GR, being less rapid for the latter (this is not evident because the figure has two different vertical scales). This comparison shows the Cowling approximation to be inaccurate for all rotation rates.

In summary, this comparison validates our approach, highlighting its accuracy and smoothness when compared to alternative methods. This will be essential to find the neutral-stability line.

## 4 RESULTS

As mentioned above, the space of parameters is spanned by the central rest-mass density and angular momentum of the rotating models. To cover the largest possible region of parameters, we have evolved 54 stellar models of relativistic stars with  $\rho_c$  in the range<sup>1</sup> [ $\rho_{\text{min}}, \rho_{\text{max}}$ ] = [ $8 \times 10^{-4}, 3.18 \times 10^{-3}$ ] and the dimensionless rotation parameter  $\beta$  between zero and the mass-shedding limit for the corresponding sequence of constant central rest-mass density ( $\beta = 0.095$  is the largest value considered). In this way, we computed stellar models with masses in the range  $M/M_{\odot} \in [1.1, 1.9]$ .

We show as the blue filled circles in Fig. 2 all of the computed F-mode frequencies, where the squares of the F-mode frequencies  $(F)^2$  are reported as a function of  $\rho_c$  and  $\beta$ . Shown as the solid magenta line is the analytic fitting of the frequency for non-rotating stars, while the dashed blue lines show sequences of rotating stars having the same rest-mass density. All models simulated have non-zero F-mode frequencies and their number diminishes for  $(F)^2 \approx 0$ . As mentioned above, this is because for these models the oscillation time-scale tends to become extremely large (diverging for  $F = 0$ ), thus becoming intractable in numerical simulations. In addition, models near the neutral point could also be artificially induced to collapse simply by the accumulation of the truncation error (see also Shibata 2003), thus preventing any reliable measure. As a result, our analysis has been constrained to values of the frequencies  $F \gtrsim 2.2 \times 10^{-3} \simeq 0.45$  kHz. Fortunately, however, the quality of the data and the smoothness in which they appear in Fig. 2 allow us to compute an analytic fit of

<sup>1</sup> Note that  $\rho_c = 1.0 \times 10^{-3} \simeq 0.62 \times 10^{15} \text{ g cm}^{-3}$  and that  $\rho_{\text{max}}$  also marks the secular-stability point for a non-rotating star.

the function  $(F)^2 = (F)^2(\rho_c, \beta)$  and thus determine analytically the neutral-stability line where  $(F)^2 = 0$ .

It is convenient to use a fitting function  $(F_{\text{fit}})^2(\rho_c, \beta)$  that is linear in  $\beta$  and  $(F_{\text{fit}})^2(\rho_{\text{max}}, 0) = 0$  by construction:

$$(F_{\text{fit}})^2(\rho_c, \beta) = (F_{\text{fit}})^2(\rho_c, 0) + \beta \sum_{n=0}^5 b_n(\rho_c)^n \quad (2)$$

$$= \sum_{n=0}^5 a_n(\rho_c)^n + \beta \sum_{n=0}^5 b_n(\rho_c)^n, \quad (3)$$

where  $a_n$  and  $b_n$  are constant coefficients, which a least-squares fitting with the data reveals to be

$$\begin{aligned} a_5 &= 6.978 \times 10^8, & a_4 &= -7.757 \times 10^6, & a_3 &= 3.621 \times 10^4, \\ a_2 &= -9.599 \times 10, & a_1 &= 1.172 \times 10^{-1}, & a_0 &= 2.110 \times 10^{-7}, \\ b_5 &= -5.599 \times 10^{10}, & b_4 &= 4.862 \times 10^8, & b_3 &= -1.612 \times 10^6, \\ b_2 &= 2.545 \times 10^3, & b_1 &= -1.896, & b_0 &= 3.357 \times 10^{-4}. \end{aligned}$$

A confirmation of the accuracy of the ansatz (3) comes from the very small variance of a comparison with perturbative results for non-rotating stars. Considering in fact over 90 stellar models with  $\rho_c \in [1.0 \times 10^{-5}, 3.182 \times 10^{-3}]$ , we obtain  $\sigma_{\text{fit}} \equiv |(F)_{\text{PT}}^2 - (F)_{\text{fit}}^2(\rho_c, 0)| \lesssim 2 \times 10^{-7} \simeq 8 \times 10^{-3} \text{ (kHz)}^2$ . Similarly, when comparing over the whole set of numerical data we find a variance that, as expected, is greater for large values of  $\rho_c$  and  $\beta$  but that, overall, is  $\sigma_{\text{fit}} \lesssim \sigma_{\text{max}} \approx 1 \times 10^{-6}$ . Note that these errors are smaller or at most comparable with the numerical error bar, highlighting the quality of the fit.

Using expression (3), it is straightforward to compute the neutral-stability line in a  $(\rho_c, \beta)$  plane as the one at which  $(F)_{\text{fit}}^2(\rho_c, \beta) = 0$ . Of course, this line will be ‘thickened’ by the uncertainty associated to the fit which, to be conservative, we consider to be  $\sigma_{\text{max}}$ . (We note that the thickness is much smaller for  $\beta \approx 0$ , but it may be larger at high  $\beta$  as a result of the extrapolation.) While a neutral-stability line is already very informative in a  $(\rho_c, \beta)$  plane, its greatest impact can be appreciated in the more traditional  $(\rho_c, M)$  diagram. This is shown in Fig. 3, where the two solid black lines refer to sequences of non-rotating (lower line) and mass-shedding models (upper line). Drawn as solid red is the neutral-stability line ‘thickened’ by the error bar  $\sigma_{\text{max}}$  (black dot–dashed lines). Finally, shown as a blue dashed line is the turning-point criterion for secular stability along a sequence of constant angular momentum  $J$ , that is,  $(\partial M / \partial \rho_c)_{J=\text{constant}} = 0$ .

Clearly, the new neutral-stability criterion does coincide with the turning-point criterion for non-rotating stars (cf. small inset), but it differs from it as the angular momentum is increased, moving to smaller central rest-mass densities. While unexpected, this difference does not point to a conflict between the two criteria. This is because the turning-point criterion is only a *sufficient* condition for secular instability of rotating stars; stated differently, while a rotating stellar model which is at or to the right-hand side of the turning-point line is expected to be also secular unstable, the opposite is not true. Hence, the two criteria are compatible as long as the secular-instability line lies to the left-hand side (i.e. for smaller central rest-mass densities) of the neutral-stability line. Determining the secular-stability line requires to consider a dissipative mechanism such as viscosity, which is, however, absent in our perfect-fluid description and difficult to introduce within a fully relativistic hyperbolic description. However, because a dynamically unstable model should also be secularly unstable, we in fact expect the secular-stability line to coincide or to be on the left-hand side of the neutral-stability line. In other words, along a  $J = \text{constant}$

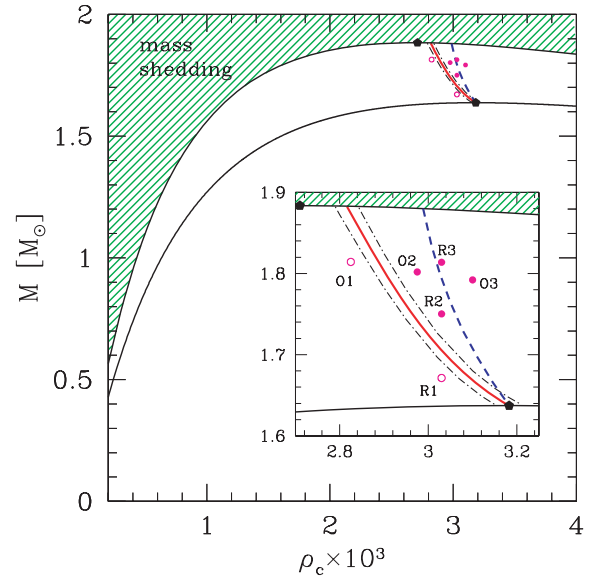


**Figure 3.** Stability lines in a  $(\rho_c, M)$  diagram. The two solid black lines mark sequences with either zero (lower line) or mass-shedding angular momentum (upper line), with the filled symbols marking the corresponding maximum masses. The solid red line is the neutral-stability line, ‘thickened’ by the error bar (black dot–dashed lines). The blue dashed line is instead the turning-point criterion for secular stability. Marked with the empty or filled circles are representative models with constant angular velocity, O1, O2 and O3, or constant initial central rest-mass density, R1, R2 and R3.

sequence of stellar models, we expect the following order with increasing rest-mass density: secular instability, dynamical instability and turning point.

To validate that the neutral-stability line should be used in place of the turning-point line to distinguish stellar models that are dynamically unstable from those that are instead stable, we have considered six representative models whose properties fall in a small region near the two stability lines. More specifically, we consider two different sequences having either constant angular velocity, that is, models O1, O2 and O3 in Fig. 4, or constant  $\rho_c$ , that is, models R1, R2 and R3. The predictions for these models are different according to which a criterion is used for stability. In fact, while models O1 and R1 are expected to be stable for both criteria and models O3 and R3 are expected to be unstable for both criteria, models O2 and R2 are predicted to be stable on a dynamical time-scale by the turning-point criterion but unstable by the neutral-stability criterion.

To test these predictions, we have evolved these configurations maintaining the same computational setup (but without an initial perturbation) and collected the corresponding evolution of the central rest-mass density in Fig. 3. As expected, models O1 and R1 are found to be stable over about 7 ms as indicated by the central rest-mass density that remains constant (modulo the F-mode oscillations), while models O3 and R3 are found to collapse to black holes in less than 2 ms as indicated by the exponential increase in the rest-mass density (see also Baiotti et al. 2005; Radice et al. 2010). Similarly, models O2 and R2 are also found to collapse to black holes over a time-scale which is only slightly larger than that of models O3 and R3. After validating that these results do not depend on the specific numerical setup used (e.g. placement of outer boundaries, resolution or density in the atmosphere), we conclude that the neutral-stability line can indeed be used to mark the boundary of a dynamically unstable region.

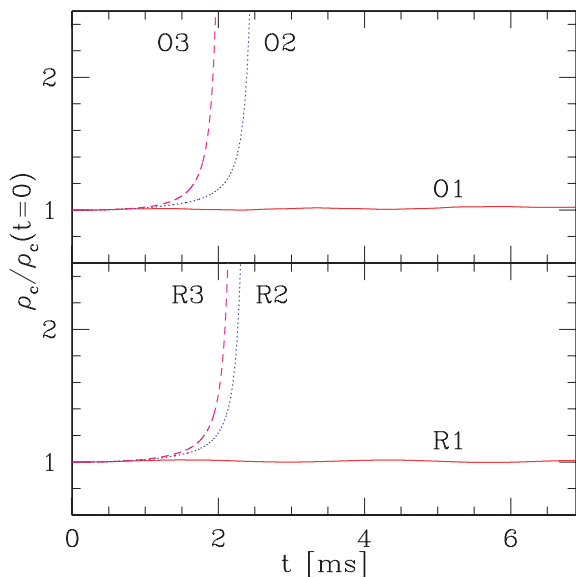


**Figure 4.** Evolution of  $\rho_c$  for models with constant angular velocity (upper panel) or constant initial central rest-mass density (lower panel). An exponential growth signals the collapse to a black hole (cf. Fig. 3).

## 5 CONCLUSIONS

The stability of rotating relativistic stars against gravitational collapse to black holes is an old problem in GR, impacting all those astrophysical problems where a neutron star may be produced and induced to collapse as a result of mass accretion. Despite the importance of this problem, no analytic criterion is known for the dynamical stability of rotating stars. Important progress was made about 20 years ago, when a criterion for secular stability was proposed by Friedman et al. (1988), who suggested that a turning point along a sequence of stellar models with constant angular momentum can be associated with the onset of secular instability. Although this criterion is only a sufficient condition for the development of a secular instability, it has been systematically used to limit the region of dynamical instability in simulations of relativistic stars (Baiotti et al. 2005; Radice et al. 2010).

To improve our understanding of the dynamical instability of relativistic stars in uniform rotation, we have computed the neutral-stability point for a large class of stellar models, that is, the set of stellar models whose F-mode frequency is vanishingly small (in a non-rotating star, this point marks the dynamical stability limit). More specifically, we have evolved in full GR 54 stellar models and calculated the corresponding F-mode frequency via a novel analysis of the PSD of the central rest-mass density. Although our simulations cannot evolve models near the neutral-stability line, the high accuracy of our estimates for the eigenfrequencies (which have been validated through a comparison with all the available data) and their regular dependence on the central rest-mass density and dimensionless rotation rate has allowed us to produce an analytic fit of the data and deduce from this the neutral-stability line. The latter coincides with the turning-point line of Friedman et al. (1988) for

non-rotating stars, but differs from it as the angular momentum is increased, being located at smaller central rest-mass densities as the angular momentum is increased. This difference does not contradict the turning-point criterion since the latter is only a sufficient condition for secular instability.

To test this result, we have evolved stellar models whose properties fall in a small region near the two stability lines, paying special attention to those stellar models that are predicted to be stable on a dynamical time-scale by the turning-point criterion but unstable by the neutral-stability line. Numerical evidence that these models do collapse to black holes allows us to conclude that the neutral-stability line can be used effectively to mark the boundary to dynamical instability. Besides improving our understanding of the stability of relativistic stars, these results show that producing black holes via the gravitational collapse of a neutron star is simpler than expected. Furthermore, they can serve as a guide when determining the neutral-stability line via perturbative techniques or when extending it to differentially rotating stars.

## ACKNOWLEDGMENTS

We are grateful to John Friedman and Nikolaos Stergioulas for extended discussions and useful suggestions that have improved the manuscript. We also thank Thorsten Kellermann for his work on the *Whisky2D* code. Support also came from the DFG grant SFB/Transregio 7 and by ‘CompStar’, a Research Networking Programme of the European Science Foundation. KT is supported by a JSPS Postdoctoral Fellowship for Research Abroad.

## REFERENCES

- Alcubierre M. et al., 2001, *Int. J. Mod. Phys. D*, 10, 273
- Baiotti L. et al., 2005, *Phys. Rev. D*, 71, 024035
- Colella P., Woodward P. R., 1984, *J. Comput. Phys.*, 54, 174
- Dimmelmeier H., Stergioulas N., Font J. A., 2006, *MNRAS*, 368, 1609
- Font J. A., Stergioulas N., Kokkotas K. D., 2000, *MNRAS*, 313, 678
- Font J. A. et al., 2002, *Phys. Rev. D*, 65, 084024
- Friedman J. L., Ipser J. R., Sorkin R. D., 1988, *ApJ*, 325, 722
- Gaertig E., Kokkotas K. D., 2008, *Phys. Rev. D*, 78, 064063
- Giacomazzo B., Rezzolla L., Baiotti L., 2009, *MNRAS*, 399, L164
- Harten A., Lax P. D., van Leer B., 1983, *SIAM Rev.*, 25, 35
- Kellerman T., Baiotti L., Giacomazzo B., Rezzolla L., 2008, *Class. Quantum Gravity*, 25, 225007
- Misner C. W., Thorne K. S., Wheeler J. A., 1973, *Gravitation*. W. H. Freeman, San Francisco
- Pollney D. et al., 2007, *Phys. Rev. D*, 76, 124002
- Radice D., Rezzolla L., Kellerman T., 2010, *Class. Quantum Gravity*, 27, 235015
- Shibata M., 2003, *Phys. Rev. D*, 67, 024033
- Stergioulas N., Friedman J. L., 1995, *ApJ*, 444, 306
- Yoshida S., Eriguchi Y., 2001, *MNRAS*, 322, 389
- Zink B., Korobkin O., Schnetter E., Stergioulas N., 2010, *Phys. Rev. D*, 81, 084055

This paper has been typeset from a  $\text{\TeX}/\text{\LaTeX}$  file prepared by the author.